# Sponge roads: the permeable asphalt pavement structures based on rainfall characteristics in central plains urban agglomeration of China

Xiaodong Guo, Jiupeng Zhang, Bochao Zhou, Wolong Liu, Jianzhong Pei and Yongsheng Guan

## ABSTRACT

Permeable asphalt pavement should be selected according to the rainfall characteristics of the project site, so as to improve the permeable performance and ensure the bearing capacity of the pavement structure. Therefore, taking a city in the central plains urban agglomeration of China as an example, the characteristics of the rainstorm intensity distribution and cumulative rainfall are analyzed, and a combination scheme of drainage surface layer asphalt pavement suitable for rainfall characteristics in this area is proposed. Then, the pavement structure design is systematically carried out based on the permeable capacity and bearing capacity. The results show that under the rainfall conditions in this area, there is no surface runoff on the permeable asphalt pavement with 120 mm drainage surface layer, which is suitable for the medium traffic grade of urban roads with cumulative equivalent axle loads of 10 million to 12 million times.

**Key words** | bearing capacity, permeable capacity, permeable pavement, sponge road, urban rainfall characteristics

**Xiaodong Guo**
**Jiupeng Zhang** (corresponding author)
**Bochao Zhou**
**Jianzhong Pei**
Key Laboratory for Special Area Highway Engineering of Ministry of Education,
Chang'an University,
Xi'an, Shaanxi 710064,
China
E-mail: *zhjiupeng@chd.edu.cn*

**Wolong Liu**
Central South Civil Aviation Airport Design and Research Institute,
Guangzhou 510080,
China

**Yongsheng Guan**
Senior Engineer Jiangsu Sinoroad Engineering Technology Research Institute Co. Ltd,
Nanjing 211800,
China

## INTRODUCTION

In recent years, dense cement concrete and dense graded asphalt mixture have occupied the main body of pavement materials. Because of the impermeability of these materials, the construction and development of cities are seriously restricted (McGrane 2016), resulting in urban floods and serious water pollution (Luo *et al.* 2019). Permeable asphalt pavement and permeable concrete pavement can alleviate such problems. Compared with ordinary pavement, this form of pavement can reduce surface runoff pollution (Wang *et al.* 2019) and effectively supplement groundwater, so it has attracted extensive attention from relevant scholars.

Permeable asphalt pavement is mainly composed of a permeable layer and an impermeable layer (Imran *et al.* 2013; Marchioni & Becciu 2018). The permeable layer is mainly responsible for the infiltration of rainwater and the filtration of surface pollutants. Because rainwater will flow along the corresponding ditches, it can also reduce the water content in the roadbed (Ghavami *et al.* 2019). The void of permeable asphalt pavement is generally greater than that of impermeable pavement, which can ensure the drainage capacity of permeable asphalt and increase the adhesion between the tire and the ground (Garcia *et al.* 2019). But excessive air voids will cause other problems, such as low strength, low stability, and poor durability. Some researches show that the permeability of permeable pavement decreases with the increase in service life of the pavement, but it can still be used (Al-Rubaei *et al.* 2013; Boogaard *et al.* 2014). The permeable layer thickness of permeable asphalt pavement is typically between 75 and 180 mm, and the design lifespan is typically around 15 years (Mullaney & Lucke 2014). When there is a higher amount of rainfall and driveway, the corresponding permeable layer should be thicker (Chai *et al.* 2012). However, with the increase in road use time, the permeable layer will cause blockage (Afonso *et al.* 2018; Selbig *et al.* 2019), which can be solved by hand-held industrial vacuum cleaning, pressure washing, and a combination of vacuum cleaning and pressure washing (Winston *et al.* 2016). In the design of permeable asphalt pavement structures in North America and other regions, the flexible pavement structure

doi: 10.2166/wst.2019.426

design guidelines in American Association of State Highway and Transportation Officials (AASHTO) are usually used (Weiss *et al.* 2019). However, different regions have different characteristics of rainfall and traffic. Unified design of urban permeable asphalt pavement may result in waste of resources or weaken the function of drainage pavement. In addition, in the process of rainfall, the rainfall is not evenly distributed, which will pose a greater challenge to the permeable asphalt pavement in places with heavy rainfall (Ball 1994). Therefore, the thickness of a structural layer designed according to the characteristics of rainfall and traffic can maximize the role of permeable asphalt pavement.

In this study, the characteristics of rainstorm intensity distribution and cumulative rainfall in some core cities of the central plains urban agglomeration in China were mainly analyzed. Taking one of them as representative, a permeable asphalt pavement suitable for rainfall characteristics in this area was proposed based on permeable and bearing capacity. It can provide some reference and guidance for the design of permeable asphalt pavement in this area and similar engineering examples in other areas.

## RAINFALL CHARACTERISTICS AND RAINSTORM INTENSITY IN CENTRAL PLAINS URBAN AGGLOMERATION

### Typical cities in central plains urban agglomeration

The central plains urban agglomeration in China mainly takes Zhengzhou, Kaifeng and Luoyang as its core development areas, leading the development of other cities. The exact location is shown in Figure 1. As an important urban agglomeration in China's future development, urban road drainage is very important. Most of the cities in the central plains urban agglomeration are of similar annual rainfall

**Figure 1** | Geographical location of Central Plains Urban Agglomeration in China.

between 400 mm and 800 mm (National Meteorological Information Center). Therefore, Zhengzhou, Kaifeng and Luoyang were taken as typical representatives of the central plains urban agglomeration to analyze the rainfall characteristics and rainstorm intensity index. The annual rainfall of three cities (National Meteorological Information Center) and their rainstorm intensity formula (Shao & Shao 2014) are shown in Table 1.

## RAINFALL CHARACTERISTICS AND RAINSTORM INTENSITY OF TYPICAL CITIES

### Rainfall characteristics in typical cities

According to the extreme rainstorms in different areas of China in recent years, a rainstorm return period of 5 years and a rain duration of 120 minutes were selected in this study. In addition, most of the rainfall in China is concentrated in the early stage. This type of rainfall will reach the peak of rainfall intensity sharply in the early stage, so the location coefficient of the rain peak is 0.35. At present, the Chicago rain pattern is widely used in the study of rainfall characteristics. The Chicago rain pattern has a good effect on the study of rainstorm characteristics in an area, and can generally meet the accuracy requirements, and there are relatively few parameters to be set. Therefore, the Chicago rain pattern was used to analyze the rainfall characteristics of the three cities in this study. Rainfall characteristics of Zhengzhou, Luoyang and Kaifeng under this condition are shown in Figure 2(a)–2(c) respectively.

It can be seen from Figure 2(a)–2(c) that the total rainfall in a continuous rainfall event in Zhengzhou, Luoyang and Kaifeng is 42.8 mm, 50.9 mm and 80.9 mm respectively, and the peak rainfall intensity at 42 minutes is 2.6 mm/min, 3.0 mm/min and 4.3 mm/min, respectively.

**Table 1** | Calculating parameters of rainstorm intensity in typical cities

| Number | Annual rainfall (mm) | Cities | Rainstorm intensity formula |
|---|---|---|---|
| 1 | 641 | Zhengzhou | $i = \frac{14.2934(1 + 0.2571\lg P)}{(t + 10.6051)^{0.7925}}$ |
| 2 | 537 | Luoyang | $i = \frac{20.0156(1 + 0.8721\lg P)}{(t + 14.8)^{0.884}}$ |
| 3 | 635 | Kaifeng | $i = \frac{4.5352(1 + 1.1280\lg P)}{(t + 3.43)^{0.5185}}$ |

Where, *i* is storm intensity (mm/min); *P* is rainstorm return period (years); *t* is rainfall duration (min).

### Rainstorm intensity index of typical cities

At present, when comparing and analyzing the characteristics of rainstorm in two cities, the peak rainfall intensity and total rainfall or rainfall characteristic curve are mainly considered. However, this method is not rigorous enough, and the results are not convincing and reliable. Therefore, two indices of rainfall intensity coefficient $\alpha$ and rainfall index $\beta$ are introduced to evaluate the variation of rainfall intensity and total rainfall in a certain rainfall period near the peak value. The calculation methods of specific $\alpha$ and $\beta$ are shown in Formulas (1) and (2).

$$\alpha = \frac{i_t}{i_0} \tag{1}$$

$$\beta = \frac{Q_t}{Q_0} \tag{2}$$

where, $\alpha$ is the rainfall intensity coefficient; $i_t$ is the minimum value of rainstorm intensity in t time period on both sides of the peak rainfall intensity (mm/min); $i_0$ is the peak rainfall intensity (mm/min); $\beta$ is the rainfall index; $Q_t$ is the cumulative rainfall in t time on both sides of the peak rainfall intensity (mm); $Q_0$ is the total rainfall in the rainstorm duration (mm).

The characteristics of urban rainfall patterns were analyzed by choosing the rainfall conditions on both sides of the peak rainfall intensity within 15 minutes in this study. The detailed analysis results are shown in Table 2.

The results show that the rainfall intensity coefficients of Zhengzhou, Luoyang and Kaifeng are all between 0.2 and 0.3, and the rainfall index are between 0.3 and 0.5. By comparing every two cities, we can find that the maximum difference of $\alpha$ and $\beta$ is about 0.1, which indicates that the region has similar rainfall characteristics.

### Analysis of urban rainfall drainage process

Generally, in a typical continuous rainfall, the characteristics of rainfall intensity can be divided into two stages; that is, the increasing stage from small value to peak value and the decreasing stage from peak value to small value. Rainwater falling on the road, if not discharged in time, will cause the accumulation of rainwater and produce surface runoff. The excessive surface runoff will cause

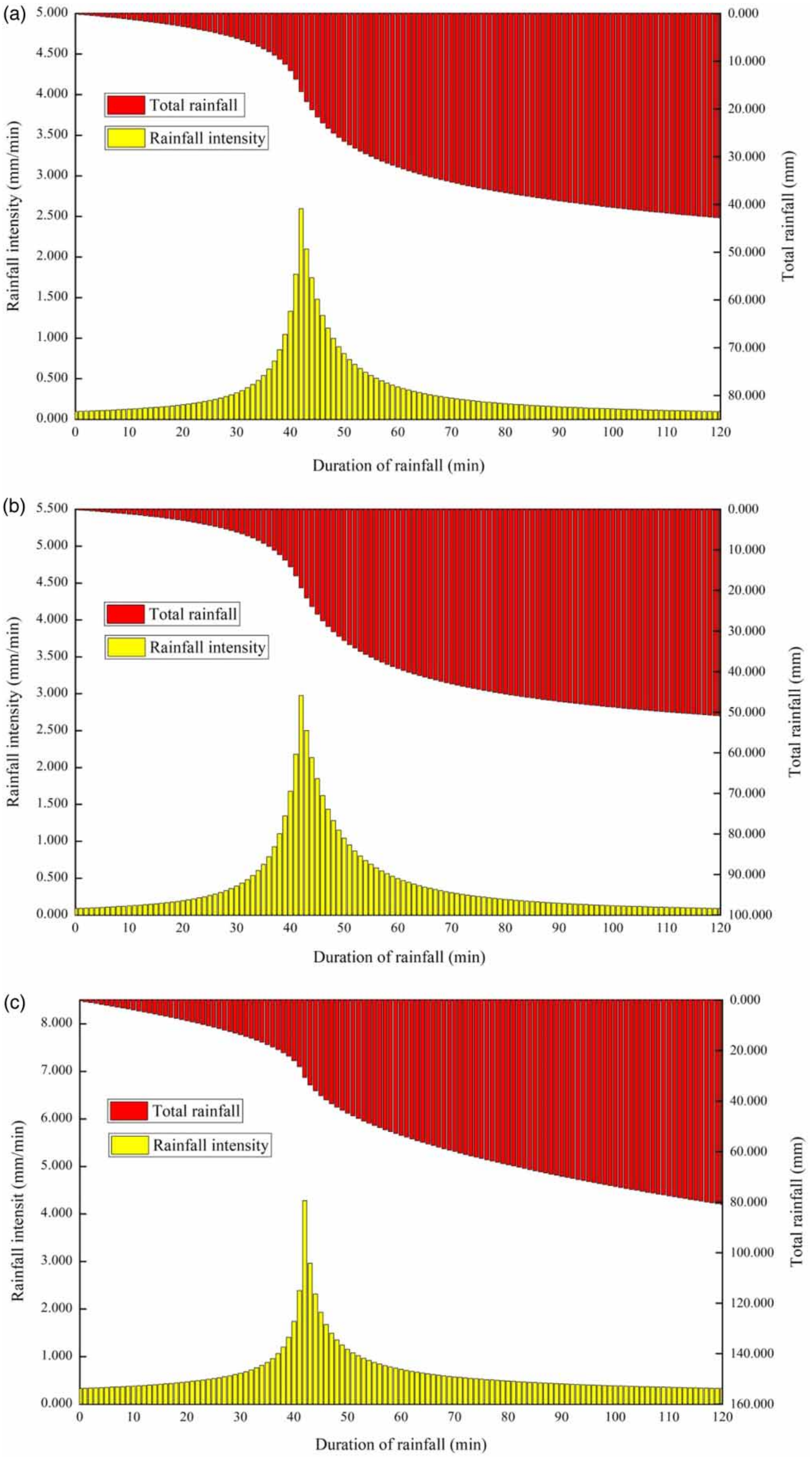

**Figure 2** | Distribution of rainfall intensity and total rainfall at different rainfall times in typical cities. (a) Zhengzhou, (b) Luoyang, (c) Kaifeng.

**Table 2** | Calculations of rainstorm characteristics in typical cities

| Cities | $i_0$ (mm/min) | $Q_0$ (mm) | $i_{15}$ (mm/min) | $Q_{15}$ (mm) | $\alpha$ | $\beta$ |
|---|---|---|---|---|---|---|
| Zhengzhou | 2.6 | 42.8 | 0.7 | 19.2 | 0.262 | 0.450 |
| Luoyang | 3.0 | 50.9 | 0.9 | 23.8 | 0.293 | 0.469 |
| Kaifeng | 4.3 | 80.9 | 1.0 | 27.0 | 0.239 | 0.334 |

pollution and urban waterlogging, and even cause serious traffic accidents. At present, there are two main ways to drain the surface runoff, one is rainwater drainage by slope or open drainage ditch, another is a permeable pavement structure to make rainwater infiltrate into the pavement structure to drain. Compared with the former, the latter can not only effectively reduce urban surface runoff, but also effectively supplement groundwater, alleviate the urban 'heat island effect' and reduce urban noise pollution.

According to Jiang Wei's research (Jiang *et al.* 2013), the process of rainwater seepage and drainage in pavement can be divided into four stages: initial pavement structure wetting, initial drainage of rainwater in the pavement structure, accumulation of rainwater in the pavement structure and drainage of rainwater from the pavement structure. Among these, rainwater storage and drainage of the pavement structure are the main processes for permeable pavement, and appropriate drainage methods should be selected according to the characteristics of the process.

## PERMEABLE ASPHALT PAVEMENT STRUCTURES WITH DRAINAGE SURFACE LAYER FOR SPONGE ROAD

### Combination design of permeable asphalt pavement structures

Permeable asphalt pavement structures mainly include three parts: surface layer, base course and roadbed, which are divided into three typical structure forms: drainage surface, permeable pavement and permeable road.

Drainage surface layer asphalt pavement refers to the pavement structure with permeable materials in the surface layer and impervious materials in the base and roadbed. This pavement structure allows rainwater to enter the surface layer and flow freely within the surface layer, eventually flowing out of the road laterally at the top of the base layer. In the whole process of rainwater seepage drainage, the base and roadbed are not affected by pavement seepage, so they are in a relatively dry environment. The whole pavement structure is of good bearing capacity and suitable for the urban environment with large traffic volumes. According to the number of drainage surface layers, this can be divided into single layer and double layer drainage structures. The specific form is shown in Figure 3(a).

Permeable road type asphalt pavement refers to the pavement structure with permeable porous materials in the surface layer and base layer, and impervious materials in the subbase and roadbed. Rainwater enters the base layer through the surface layer and flows freely within the base layer, eventually flowing out from the side along the top of the subbase. In this process, the roadbed is completely unaffected by the infiltration of rainwater into the pavement. The roadbed is in a dry environment. Therefore, the pavement structure is of a good bearing capacity and suitable for the urban environment with moderate traffic volumes and heavy rainfall intensity. The specific form is shown in Figure 3(b).

Permeable road asphalt pavement refers to the pavement structure with permeable materials on the surface, base, subbase and roadbed. This kind of permeable asphalt pavement can ensure that the rainwater enters the surface layer and seeps into the roadbed through the base, and finally replenishes groundwater to realize the recycling of water resources within the city. However, the bearing capacity of this structure is poor, so it is only suitable for the urban environment with small traffic volumes and heavy rainfall intensity. The specific form is shown in Figure 3(c).

According to the geographical location of the central plains urban agglomeration, the annual rainfall of most cities is between 400 mm and 800 mm, and the rainfall intensity is moderate, while the traffic volume of the core urban areas such as Zhengzhou, Kaifeng and Luoyang is large. Therefore the drainage surface layer asphalt pavement is adopted as the structure of pavement in this area.

## EFFECTS OF PERMEABLE SURFACE LAYER THICKNESS ON PERMEABILITY OF SPONGE ROAD

### Permeability analysis by using SWMM

The rainstorm flood management model was first developed by the US Environmental Protection Agency in the 1970s as a comprehensive mathematical model for urban rainwater design and management. It can dynamically simulate the whole urban rainfall-runoff process, including surface runoff, drainage pipeline transportation and

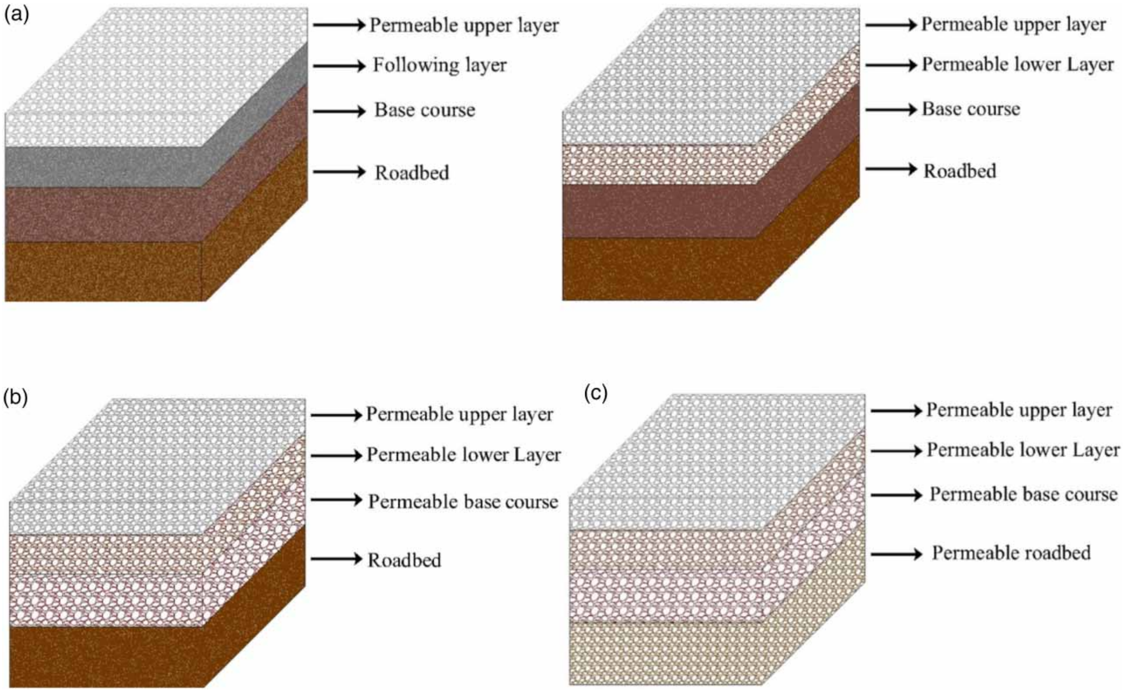

**Figure 3** | Typical structure of permeable asphalt pavement. (a) Drainage surface layer asphalt pavement (single layer, double layer). (b) Permeable road type asphalt pavement. (c) Permeable road asphalt pavement.

rainwater convergence. At the same time, the problem of water quality in the urban drainage system can be solved.

The Stormwater Management Model (SWMM) is used to simulate the effect of different thicknesses of drainage asphalt pavement on the peak flow of urban rainfall in this study. Through the numerical analysis of drainage structure layer thickness and cumulative surface runoff, the functional relationship between them is established, and then the total design thickness of the drainage structure layer is calculated when there is no surface runoff. The specific simulation flow of the permeability analysis of a drainage asphalt pavement in the SWMM model is shown in Figure 4.

## Permeable pavement sub-catchment area

Zhengzhou, the core city of the central plains urban agglomeration in China, was selected as a representative city to carry out the design and analysis of drainage surface layer asphalt pavement. It is assumed that the total length of the road paved with drainage asphalt pavement in a certain area of the city is 500 m, the central green belt is 2 m wide in the middle of the road, and the motor lane (two-way six-lane) is 10.5 m wide on both sides. This study only considered the drainage of rainwater falling to permeable asphalt pavement, the rainfall infiltration of greenbelt is not the focus; that is, the division of the sub-catchment area of greenbelt is not carried out. Assuming that each box represents a sub-catchment area, the motor lane of the road can be divided into 10 sub-catchment areas, each with a length of 100 m and width of 10.5 m. Each side of the motor lane contains five sub-catchment areas. The sub-catchment areas drawn by storm runoff simulation software SWMM5.1 are shown in Figure 5.

## Pavement drainage parameters

When researching the structure of drainage surface layer asphalt pavement suitable for rainfall characteristics in

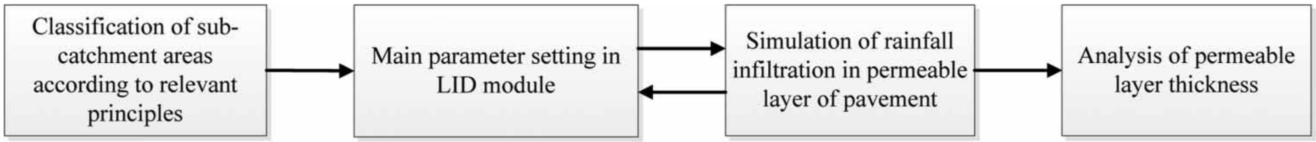

**Figure 4** | Flow chart of permeable pavement simulation in SWMM model.

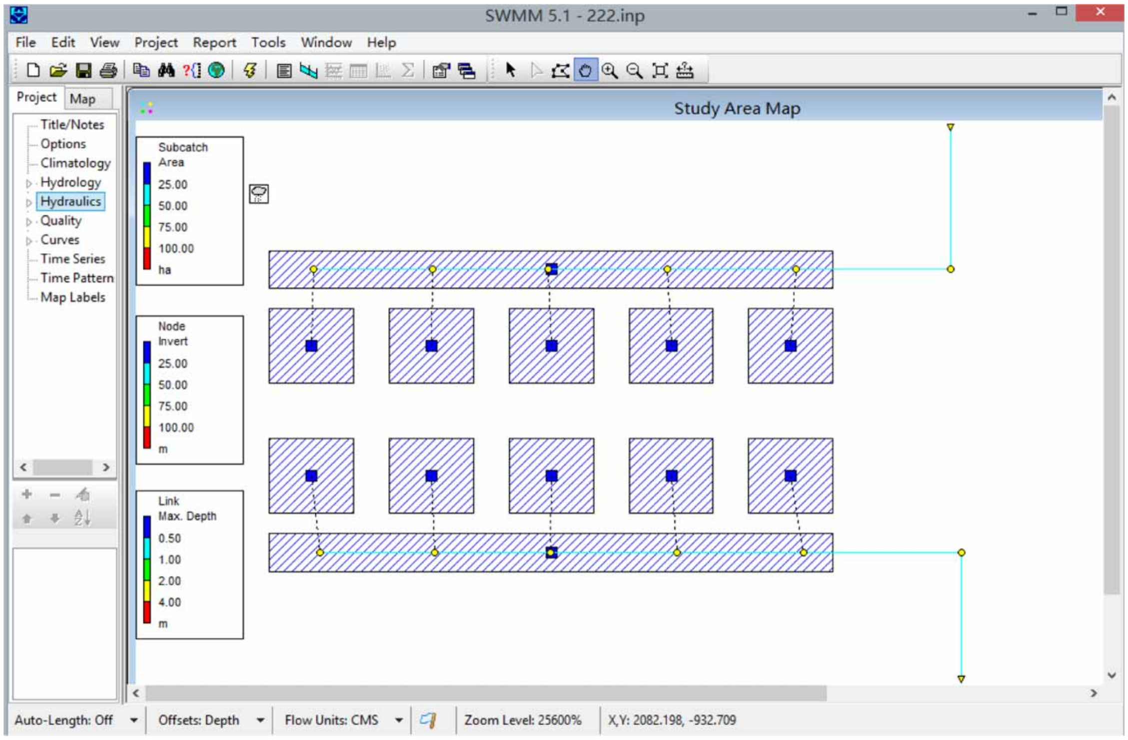

Auto-Length: Off | Offsets: Depth | Flow Units: CMS | Zoom Level: 25600% | X,Y: 2082.198, -932.709

**Figure 5** | Distribution of sub-catchments in the study area.

Zhengzhou, the void ratio of surface drainage material is set to 20%. Referring to 'Technical Specification for Permeable Asphalt Pavement' (CJJ/T 190-2012) (CJJ 2012) and relevant literature (Jiang 2011), the specific parameters can be set as shown in Table 3.

## Analysis of simulation results

The pervious capacity of different thicknesses of pervious pavement is different. In the process of a rainfall event, it is possible for surface runoff to be generated while the infiltration capacity is not exceeded due to limitations imposed by the hydraulic conductivity of the pavement structure (Rankin & Ball 2010). In this case, according to the rainfall characteristics of Zhengzhou, the thickness of the drainage asphalt surfaces was 40 mm, 50 mm, 60 mm, 70 mm and 80 mm. The total amount of surface runoff and the water storage height of the pavement structure under different drainage surface thicknesses are calculated by using the simulation software SWMM5.1. The concrete calculation results are shown in Table 4 and Figure 6.

Where, H is drainage surface thickness; $Q_0$ is total rainfall; $\gamma$ is pavement seepage drainage ratio; t is starting time of surface runoff; $H_0$ is maximum storage height of the drainage layer.

From Table 4 and Figure 6, it can be seen that with the increase of the total thickness of drainage surface, the total amount of surface runoff decreases gradually, the starting

**Table 3** | Main setting parameters of drainage surface layer asphalt pavement

| Surface layer | Range of values | Permeable layer | Range of values |
|---|---|---|---|
| Equivalent water storage depth/mm | 0.015H | Thickness/mm | H |
| Vegetation coverage coefficient | 0 | Void ratio | 0.18 |
| Surface roughness coefficient | 0.015 | Impermeability coefficient | 0 |
| Surface gradient | 2.0 | Permeability/(mm/min) | 258 |
| | | Blocking factor | 0 |

**Table 4** | Simulation results under different drainage surface thicknesses

| Number | H/mm | $Q_0$/mm | Q/mm | $\gamma$/% | t/min | $H_0$/mm |
|---|---|---|---|---|---|---|
| 1 | 40 | 42.8 | 20.4 | 47.84 | 41 | 40 |
| 2 | 50 | 42.8 | 17.0 | 39.76 | 42 | 50 |
| 3 | 60 | 42.8 | 13.6 | 31.77 | 43 | 60 |
| 4 | 70 | 42.8 | 10.5 | 24.54 | 45 | 70 |
| 5 | 80 | 42.8 | 7.7 | 17.88 | 48 | 80 |

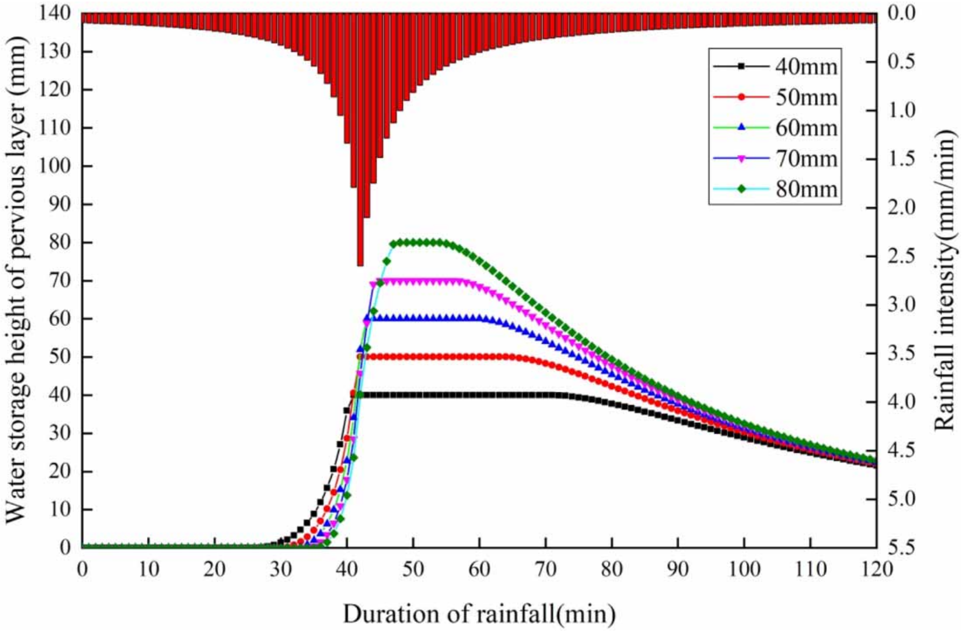

**Figure 6** | Calculating results of surface runoff under different drainage surface thicknesses.

time of surface runoff delays gradually, and the maximum impoundment height in the pavement structure increases gradually. It shows that increasing the thickness of the drainage structure layer can effectively reduce the total amount of surface runoff and delay the time of surface runoff. Combining Table 4 and Figure 6, it can be seen that no surface runoff can be generated on urban roads in rainstorm days by changing the total design thickness of the drainage structure layer. Based on this assumption, this study fitted and analysed the thickness of the drainage surface layer and the total amount of surface runoff in Table 4. From the results of numerical fitting, the total design thickness of a drainage surface layer that satisfies the characteristics of urban rainstorms in Zhengzhou without surface runoff can be obtained. The specific analysis results are shown in Figure 7.

From Figure 7, it can be seen that according to the characteristics of urban rainstorms in Zhengzhou, there is a negative correlation between the thickness of the drainage layer and the total amount of surface runoff. The fitting curve is an exponential function curve. The formula obtained by fitting analysis is shown in Formula (3).

$$Q = 55.92e^{-\frac{H}{80.94}} - 13.09\,R^2 = 0.9456 \tag{3}$$

According to Formula (3), when the total amount of surface runoff is zero, the total design thickness of drainage surface layer is 117.48 mm; that is, the total design thickness of the drainage surface layer that satisfies the characteristics of the urban rain pattern in Zhengzhou and has no surface runoff is 120 mm.

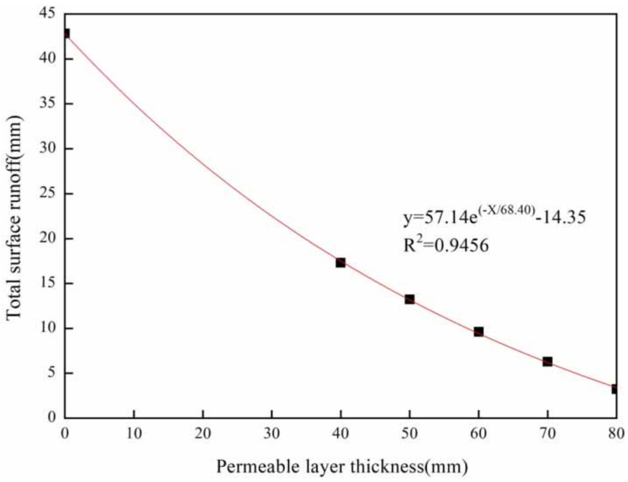

**Figure 7** | Fitting analysis of drainage surface thickness and total surface runoff.

## EFFECT OF PERMEABLE SURFACE THICKNESS ON BEARING CAPACITY OF SPONGE ROAD

### Material parameters of structural layer

Previous calculation showed that the total design thickness of drainage surface satisfying the characteristics of urban rainstorms in Zhengzhou is 120 mm. In this section, the bearing capacity design of the drainage surface layer asphalt pavement structure was analysed by BISAR 3.0. The material parameters of each structural layer were selected according to 'Technical Specification for Permeable Asphalt Pavement' (CJJ/T 190-2012) (CJJ 2012) and relevant literature (Jiang 2011); they are shown in Table 5.

## Analysis of calculation results

Based on the selection of materials and determination of design parameters for each structural layer of drainage surface layer asphalt pavement, the surface deflection, maximum tensile stress at the bottom of the asphalt surface and maximum tensile stress at the bottom of the semi-rigid base layer of the drainage surface layer asphalt pavement with different thickness combinations of drainage surface layer were analyzed by BISAR 3.0. The concrete calculation results are shown in Table 6.

Table 6 shows that, under the same thickness as other structural layers of the pavement, with the increase in the total thickness of the drainage surface, the surface deflection, the maximum tensile stress at the bottom of the asphalt surface layer and the maximum tensile stress at the bottom of the semi-rigid base layer decrease gradually. It shows that reasonable distribution of drainage surface thickness can effectively improve the overall bearing capacity of the pavement. At the same time, increasing the total design thickness of the drainage surface can also improve the overall bearing capacity of drainage surface layer asphalt pavement.

**Table 5** | Material parameters of pavement structural layers

| Layer materials | 20 °C compressive resilient modulus/ MPa | Poisson's ratio | Layer thickness/ mm |
|---|---|---|---|
| PAC-13 | 700 | 0.25 | – |
| PAC-20 | 700 | 0.25 | – |
| Inorganic binder stabilized macadam | 1,500 | 0.25 | 250 |
| Inorganic binder stabilized soil | 800 | 0.25 | 300 |
| Subgrade soil | 40 | 0.35 | – |

**Table 6** | Main indicators of asphalt pavement with different thicknesses of drainage layer

| | h/mm | | | | |
|---|---|---|---|---|---|
| Number | Upper layer | Lower layer | $l_s$/0.01 mm | $\sigma_{m1}$/MPa | $\sigma_{m2}$/MPa |
| 1 | 50 | 70 | 47.04 | 0.253 | 0.098 |
| 2 | 50 | 80 | 47.04 | 0.216 | 0.098 |
| 3 | 50 | 90 | 46.36 | 0.248 | 0.093 |
| 4 | 50 | 100 | 45.70 | 0.238 | 0.088 |
| 5 | 50 | 110 | 45.70 | 0.206 | 0.085 |

Where, h is drainage layer thickness; $l_s$ is surface deflection; $\sigma_{m1}$ is maximum tensile stress at the bottom of the asphalt pavement; $\sigma_{m2}$ is maximum tensile stress at the bottom of the semi-rigid base layer.

According to the literature to determine the relevant parameters and calculate the pavement structure design indicators, the calculation results for the relevant design indicators are shown in Table 7.

Comparing the values of Table 6 with the main design indexes of Table 7, it can be seen that the cumulative equivalent axle loads applicable to the drainage asphalt pavement structure range from 6 million to 7 million, which belongs to the category of medium traffic grade of urban roads, and this is the area with smaller values, so its applicable traffic conditions are relatively low. Further research shows that when all the surface layers of the pavement structure are pervious layers, considering the deflection value of the pavement surface as the design index, the bearing capacity of the whole pavement is low and can not meet the urban road environment of a larger traffic grade. Therefore, considering the total thickness of pervious surface layer that meets the drainage requirements of urban rainstorm characteristics, a lower layer paved with compact asphalt mixture can be added. This can effectively improve the overall bearing capacity of drainage surface layer asphalt pavement.

On the premise of keeping the thickness of other pavement structural layers unchanged, this study explored the influence of adding a lower paved layer of compact asphalt mixture on the overall bearing capacity of the drainage

**Table 7** | Main design indexes of asphalt pavement with different traffic volumes (Jiang 2011)

| Traffic grade | $N_e$/times | $l_d$/0.01 mm | $\sigma_{R1}$/MPa | $\sigma_{R2}$/MPa |
|---|---|---|---|---|
| Medium traffic | 5.00E + 6 | 52.68 | 0.29 | 0.35 |
| | 6.00E + 6 | 50.80 | 0.28 | 0.34 |
| | 7.00E + 6 | 45.15 | 0.25 | 0.31 |
| | 8.00E + 6 | 43.96 | 0.24 | 0.30 |
| | 9.00E + 6 | 42.94 | 0.23 | 0.30 |
| | 1.00E + 7 | 42.04 | 0.23 | 0.29 |
| | 1.10E + 7 | 41.25 | 0.22 | 0.29 |
| | 1.20E + 7 | 40.53 | 0.22 | 0.29 |

Where, $N_e$ is cumulative equivalent axle loads; $l_d$ is design deflection of road surface; $\sigma_{R1}$ is permissible tensile stress at the bottom of the asphalt surface; $\sigma_{R2}$ is permissible tensile stress at the bottom of the semi-rigid base layer.

**Table 8** | Design indicators of drainage asphalt pavement

| | h/mm | | | | |
|---|---|---|---|---|---|
| **Number** | **Upper and middle layers** | **Lower layer** | **$l_s$/0.01 mm** | **$\sigma_{m1}$/MPa** | **$\sigma_{m2}$/MPa** |
| 1 | 50 + 70 | 70 | 41.54 | 0.226 | 0.077 |
| 2 | 50 + 70 | 80 | 41.23 | 0.215 | 0.074 |
| 3 | 50 + 80 | 80 | 40.95 | 0.213 | 0.072 |

surface layer asphalt pavement selected previously. The concrete calculation results are shown in Table 8.

Combined with Tables 7 and 8, it can be seen that by laying a certain thickness of compact asphalt mixture as the lower layer, its applicable cumulative equivalent axle load times range from 10 million to 12 million, which belongs to the category of medium traffic grade of urban roads. Comparing the relevant data in Tables 6 and 8, it can be concluded that laying the appropriate thickness of compact asphalt mixture as the lower layer can greatly improve the bearing capacity of the whole permeable asphalt pavement. Therefore, under the premise of ensuring that the thickness of the permeable layer of the pavement meets the drainage requirements, we can consider adding a certain thickness of dense asphalt mixture as the lower layer.

## CONCLUSION

In this study, the typical cities of the central plains urban agglomeration in China were analyzed. The core city of Zhengzhou was taken as the representative to analyze the characteristics of rainstorm and design the drainage and carrying capacity. The main conclusions are as follows:

(1) Rainfall characteristics of the central plains urban agglomeration with Zhengzhou, Kaifeng and Luoyang as the core cities are similar. Drainage surface layer asphalt pavement can be used to design drainage structure in this area.

(2) The cumulative total rainfall in Zhengzhou is 42.8226 mm, and the peak rainfall intensity is 2.5984 mm/min at 42 minutes; when the rainstorm return period is 5 years, the duration of rainfall is 120 minutes and the location coefficient of the rain peak is 0.35.

(3) Using SWMM5.1 to simulate and analyze the urban road rainwater seepage drainage in Zhengzhou, it is concluded that the minimum design thickness of drainage surface layer that meets the requirements of road drainage in this area should be 120 mm.

(4) The pavement structure of drainage surface layer asphalt pavement with different drainage layer thicknesses was analyzed by BIASR3.0. It is concluded that the accumulative equivalent axle loads of drainage surface layer asphalt pavement designed under rainfall characteristics in this area ranges from 10 million to 12 million times, which belongs to medium traffic grade of urban road.

## ACKNOWLEDGEMENTS

This work was supported by National Key R&D Program of China (No. 2018YFE0103800), China Postdoctoral Science Foundation (No. 2017M620434), Shaanxi Postdoctoral Grant Program (No. 2017BSHYDZZ17), the Special Fund for Basic Scientific Research of Central College of Chang'an University (No. 310821173501), and Jiangsu International Science and Technology Cooperation Project (BZ2017011). The authors gratefully acknowledge their financial support.

## REFERENCES

Afonso, M. L., Fael, C. S. & Dinis-Almeida, M. 2018 Influence of clogging on the hydrologic performance of a double layer porous asphalt. *International Journal of Pavement Engineering* 1–10. doi:10.1080/10298436.2018.1508843.

Al-Rubaei, A. M., Stenglein, A. L., Viklander, M. & Blecken, G. T. 2013 Long-term hydraulic performance of porous asphalt pavements in northern Sweden. *Journal of Irrigation and Drainage Engineering* **139** (6), 499–505. doi:10.1061/(asce)ir.1943-4774.0000569.

Ball, J. E. 1994 The influence of storm temporal patterns on catchment response. *Journal of Hydrology* **158** (3/4), 285–303. doi:10.1016/0022-1694(94)90058-2.

Boogaard, F., Lucke, T. & Beecham, S. 2014 Effect of age of permeable pavements on their infiltration function. *CLEAN – Soil, Air, Water* **42** (2), 146–152. doi:10.1002/clen.201300113.

Chai, L., Kayhanian, M., Givens, B., Harvey, J. T. & Jones, D. 2012 Hydraulic performance of fully permeable highway shoulder for storm water runoff management. *Journal of Environmental Engineering* **138** (7), 711–722. doi:10.1061/(asce)ee.1943-7870.0000523.

CJJ/T 190-2012 2012 *Technical Specification for Permeable Asphalt Pavement*. China Architecture & Building Press, Beijing.

Garcia, E. S., Thives, L. P., Ghisi, E. & Antunes, L. N. 2019 Analysis of permeability reduction in drainage asphalt mixtures due to decrease in void volume. *Journal of Cleaner Production* 119292. doi:10.1016/j.jclepro.2019.119292.

Ghavami, M. S. M., Hosseini, M. S., Zavattieri, P. D. & Haddock, J. E. 2019 Flexible pavement drainage system effectiveness. *Construction and Building Materials* **218**, 99–107. doi:10.1016/j.conbuildmat.2019.05.088.

Imran, H. M., Akib, S. & Karim, M. R. 2013 Permeable pavement and stormwater management systems: a review. *Environmental Technology* **34** (18), 2649–2656. doi:10.1080/09593330.2013.782573.

Jiang, W. 2011 *Composition Design and Functional Evaluation For Materials and Structures of Permeable Asphalt Pavement*. Chang'an University.

Jiang, W., Sha, A., Xiao, J. & Pei, J. 2013 Water storage-infiltration model for permeable asphalt pavement and its efficiency. *Journal of Tongji University. Natural Science* **41** (1), 72–77.

Luo, P., Kang, S., Zhou, M., Lyu, J., Aisyah, S., Binaya, M. & Nover, D. 2019 Water quality trend assessment in Jakarta: a rapidly growing Asian megacity. *PLoS One* **14** (7), e0219009. doi:10.1371/journal.pone.0219009.

Marchioni, M. & Becciu, G. 2018 Infiltration-exfiltration system for stormwater runoff volume and peak attenuation. *International Journal of Safety and Security Engineering* **8** (4), 473–483. doi:10.2495/SAFE-V8-N4-473-483.

McGrane, S. J. 2016 Impacts of urbanization on hydrological and water quality dynamics, and urban water management: a review. *International Association of Scientific Hydrology. Bulletin* **61** (13), 17. doi:10.1080/02626667.2015.1128084.

Mullaney, J. & Lucke, T. 2014 Practical review of pervious pavement designs. *CLEAN–Soil, Air, Water* **42** (2), 111–124. doi:10.1002/clen.201300118.

National Meteorological Information Center. Available from http://data.cma.cn/en (accessed 10 December 2019).

Rankin, K. & Ball, J. E. 2010 The hydrologic performance of permeable pavers. *Urban Water* **7** (2), 79–90. doi:10.1080/15730620902969773.

Selbig, W. R., Buer, N. & Danz, M. E. 2019 Stormwater-quality performance of lined permeable pavement systems. *Journal of Environmental Management* **251**, 109510. doi:10.1016/j.jenvman.2019.109510.

Shao, Y. & Shao, D. 2014 *A New Generation of Urban Rainstorm Intensity Formula in China*. China Architecture & Building Press, Beijing, China.

Wang, H., Li, H., Liang, X., Zhou, H., Xie, N. & Dai, Z. 2019 Investigation on the mechanical properties and environmental impacts of pervious concrete containing fly ash based on the cement-aggregate ratio. *Construction and Building Materials* **202**, 387–395. doi:10.1016/j.conbuildmat.2019.01.044.

Weiss, P. T., Kayhanian, M., Gulliver, J. S. & Khazanovich, L. 2019 Permeable pavement in northern North American urban areas: research review and knowledge gaps. *International Journal of Pavement Engineering* **20** (2), 143–162. doi:10.1080/10298436.2017.1279482.

Winston, R. J., Al-Rubaei, A. M., Blecken, G. T., Viklander, M. & Hunt, W. F. 2016 Maintenance measures for preservation and recovery of permeable pavement surface infiltration rate – the effects of street sweeping, vacuum cleaning, high pressure washing, and milling. *Journal of Environmental Management* **169**, 132–144. doi:10.1016/j.jenvman.2015.12.026.

First received 18 August 2019; accepted in revised form 12 December 2019. Available online 24 December 2019